CopERnIcus climate change Service Evolution

D2.4 Documentation of coupled skin temperature assimilation for regional reanalysis

Due date of deliverable	31st December 2025
Submission date	18th December 2025
File Name	CERISE-D2.4-V1.0
Work Package /Task	WP2 Task 2.3
Organisation Responsible of Deliverable	SMHI
Author name(s)	Jelena Bojarova, Mehdi Eshagh, José Manuel Faúndez Alarcon, Jostein Blyverket, Åsmund Bakketun
Revision number	V1.0
Status	ISSUED
Dissemination Level	PU

Funded by the European Union

The CERISE project (grant agreement No 101082139) is funded by the European Union.
Views and opinions expressed are however those of the author(s) only and do not necessarily reflect those of the European Union or the Commission. Neither the European Union nor the granting authority can be held responsible for them.

1 Executive Summary

This report summarises the developments made in the Copernicus Climate Change Service Evolution (CERISE) project towards a unified ensemble-based data assimilation (DA) framework for regional reanalysis applications. This project focuses on improving the treatment of soil and surface variables across various temporal and spatial scales, which is essential for enhancing the accuracy of regional reanalysis products. Also, it addresses three primary areas of development:

1. One key aim of CERISE is to standardise the analysis of snow and soil variables, which are currently treated using different methods. This inconsistency leads to challenges in the quality of the reanalysis products and increases the maintenance burden. The project aims to create a more unified approach to improve the consistency and quality of these analyses.
2. CERISE also focuses on developing flexible ensemble-based DA techniques for the interaction soil biosphere atmosphere (ISBA, Noihan and Mahfoof 1996) soil model and the multi-layer snow scheme. By incorporating advanced physical models and flexible DA methods, CERISE seeks to improve the assimilation of diverse observations from various platforms, ultimately enhancing the quality of near-surface variable reanalysis products.
3. CERISE takes important steps towards the development of a consistent hydrological-meteorological forecasting system that accounts for the full evolution of the water cycle, including snow and surface-atmosphere interactions.

The work has been carried out by three teams, each contributing to the integration of the developed methods into the High-Resolution Limited Area Model – Applications of Research to Operations at Mesoscale (HARMONIE-AROME, Seity et al. 2011, Bengtsson et al. 2017) code.

- The Swedish Meteorological and Hydrological Institute (SMHI) team has focused on the development of ensemble square root Kalman filter (EnSRKF, Tippett et al. 2003) in the inline HARMONIE-Arome environment. It improves the propagation of information from surface-level variables into the soil, producing analyses that align more closely with observations. A comparison with the simplified extended Kalman filter (sEKF) scheme has demonstrated improvements in soil variable analysis. The SMHI team has focused as well on improving coupling functionalities to obtain a more consistent exchange of information between the land surface and the atmosphere. This is done both through the development of the land surface atmosphere coupling within the outer-loop 4DVAR and through implementation of skin temperature analysis through extended control variable approach.
- The Met Norway team has concentrated on the development of a local ensemble transform Kalman filter (LETKF, Hunt el a. 2007) for assimilating surface temperature and snow depth data, using satellite sensor data from advanced microwave sounding unit A and B *(*AMSU-A and AMSU-B) in an offline environment. LETKF has proven effective in treating the satellite footprint in a localised manner, significantly improving snowpack estimates, particularly in flat orographic regions.
- The SMHI hydrological team has worked on improving snow DA by developing an ensemble Kalman filter approach. Special focus has been given to the snow memory and its proper treatment over the timescales of numerical weather prediction (NWP) models.

The CERISE project places a strong emphasis on integrating coupled skin temperature assimilation to enhance the representation of surface-atmosphere interactions, a crucial advancement in improving the prediction and analysis of near-surface variables.

Table of Contents

2 Introduction

Accurate regional numerical weather prediction (NWP) relies on advanced models that simulate interactions between the atmosphere, oceans, land surface, and other Earth system components. Skin temperature (SKT) plays a key role in processes like heat exchange, moisture flux, and energy balance. Integrating real-world SKT data into NWP models through coupled SKT assimilation refines predictions by aligning them with observed data, allowing the models to better capture surface-atmosphere interactions and improving performance. This technique is especially useful in regional reanalysis, where it combines observational data with model simulations to create consistent, long-term climate datasets for specific areas, enhancing our understanding of local weather patterns, extreme events, and climate trends. Such an approach is crucial for applications in regional climate monitoring, agriculture, hydrology, and disaster management, providing accurate, localised climate information that informs climate change predictions and policy decisions.

Work Package 2 (WP2) of CopERnIcus climate change Service Evolution (CERISE) project aims to develop advanced coupled surface-atmosphere assimilation methods to enhance the representation of SKT and other surface variables within both regional and global reanalysis systems. Building on recent advancements in ocean-atmosphere coupling. It will focus on harmonising strategies for land-atmosphere and ocean-atmosphere assimilation, including the integration/assimilation of SKT data from satellite observations, which will be incorporated into the atmospheric four-dimensional variational data assimilation (DA) (4D-Var Thépaut et al. 1991) system. This method will better constrain important land surface variables such as snow, soil, and sea ice temperatures, ultimately improving the accuracy of surface-atmosphere interactions in the models. Also, WP2 will explore various degrees of coupling between the land surface and atmosphere, aiming to identify the optimal configuration for initialising surface-atmosphere variables, including SKT, across both regional and global systems. The assimilation system will also integrate land surface and atmospheric observation operators, enabling a more holistic, all-sky, all-surface approach. This will allow for the simultaneous analysis of SKT and other surface variables, improving the representation of surface-atmosphere feedbacks in the model. Furthermore, incorporating SKT into these coupled assimilation systems is crucial for enhancing model performance in challenging environments, such as snow-covered regions and warm deserts, where surface-atmosphere interactions are particularly sensitive. WP2's developments will support regional reanalysis efforts, providing more accurate datasets for local weather patterns and climate trends, which will have significant applications in climate monitoring, agriculture, hydrology, and disaster management. These advancements will ultimately lead to more precise predictions of climate change impacts and better-informed policy decisions.

In this deliverable, after presenting the backgrounds in Section 1.1, the scope of the deliverable, containing the objectives, the performed work, and deviation and counter measures as well as the reference document are presented in Section 1.2.

2.1 Background

The scope of CERISE is to enhance the quality of the Copernicus climate change service (C3S) reanalysis and seasonal forecast portfolio, with a focus on land-atmosphere coupling. It will support the evolution of C3S, over the project's four year timescale and beyond, by improving the C3S climate reanalysis and the seasonal prediction systems and products towards enhanced integrity and coherence of the C3S Earth system essential climate variables. CERISE will develop new and innovative ensemble-based coupled land-atmosphere DA approaches and land surface initialisation techniques to pave the way for the next generations of the C3S reanalysis and seasonal prediction systems.

These developments will be combined with innovative work on observation operator developments integrating artificial intelligence (AI) to ensure optimal data fusion fully integrated in coupled assimilation systems. They will drastically enhance the exploitation of past, current, and future Earth system observations over land surfaces, including from the Copernicus Sentinel satellite missions and from the European space agency (ESA) Earth explorer missions, moving towards an all-sky and all-surface approach. For example, land observations can simultaneously improve the representation and prediction of land and atmosphere and provide additional benefits through the coupling feedback mechanisms. Using an ensemble-based approach will improve uncertainty estimates over land and lowest atmospheric levels. By improving coupled land-atmosphere assimilation methods, land surface evolution, and satellite data exploitation, research and innovation inputs from CERISE will improve the representation of long-term trends and regional extremes in the C3S reanalysis and seasonal prediction systems.

In addition, CERISE will provide proof of concept demonstrating the feasibility of integrating the developed approaches into the core C3S operational service. This will be achieved through the delivery of reanalysis prototype datasets (demonstrated in a pre-operational environment) and seasonal-prediction demonstrator datasets in a relevant environment. CERISE will also enhance the quality and consistency of the C3S reanalysis systems and the components of the seasonal-prediction multi-system, directly addressing evolving user needs for improved and more coherent C3S Earth system products.

2.2 Scope of this deliverable

This report focuses on the development and application of coupled surface-atmosphere assimilation methods within the framework of C3S regional reanalysis systems. The primary objective is to explore and implement innovative techniques that improve the assimilation of surface-sensitive observations, specifically those related to SKT and other land surface variables, in both global and regional reanalysis systems.

As part of the CERISE project, this deliverable outlines the evolution of the C3S regional reanalysis infrastructure, including the development of advanced ensemble-based coupled land-atmosphere DA methods. These methods aim to enhance the representation and prediction of surface-atmosphere interactions, particularly by integrating data from the Copernicus Sentinel satellites and ESA Earth Explorer missions.

The report covers the improvement of surface-sensitive observations utilisation, focusing on how coupling these observations can lead to better predictions of regional climate extremes, long-term trends, and variability in snow-covered regions. Additionally, it will present the potential for these developments to provide more accurate reanalysis datasets prototypes that can address evolving user needs for more consistent and reliable Earth system products.

2.2.1 Objectives of this deliverables

The primary objective of this deliverable is to present the advancements made in the development and implementation of coupled SKT assimilation methods for improving the C3S reanalysis and seasonal forecast systems. This deliverable aims to:

- To introduce novel ensemble-based coupled land-atmosphere DA techniques, like EnSRKF and LETKF, that enhance the accuracy and efficiency of regional reanalysis systems. These methods will allow for better representation of surface-atmosphere interactions, with a particular focus on SKT and surface variables.

- To enhance the utilisation of surface-sensitive observations, including satellite-derived data from Copernicus Sentinel missions and ESA Earth explorer missions, within the coupled assimilation framework. The goal is to integrate these observations in a way that improves both the initialisation and long-term prediction of land surface and atmospheric variables.

2.2.2 Work performed in this deliverable

The work performed in this deliverable has focused on exploring different approaches to obtain powerful yet affordable solutions. The aim is to enhance the quality of the new-generation reanalysis product, with particular emphasis on land–atmosphere coupling when constructing the initial conditions for the forward model integration. After presenting the CERISE project partners in Section 2, Section 3 provides an overview of the SKT variables and offers insights into assimilation performance. Subsection 3.1 discusses the treatment of SKT variables in the atmosphere and surface forecasting system and describes the challenges associated with implementing coupled SKT assimilation in the Harmonie-Arome system. Subsection 3.2 examines the performance of the surface DA scheme, presenting insights gained from stand-alone experiments.

Section 4 addresses the weakly coupled DA of AMSR2 brightness temperatures and describes the implementation of this approach together with its impact on analysis quality. Section 5 discusses outer-loop 4D-Var land–atmosphere coupling and evaluates the ability of the outer-loop 4D-Var system to exchange information between the atmospheric and land models. Section 6 introduces the extended control variable approach and presents the implementation of coupled surface-temperature DA based on this method. Conclusions are summarised in Section 7.

2.2.3 Deviations and counter measures

No deviations have been encountered during the reporting period. All processes, results, and operational metrics are currently aligned with the planned objectives and established thresholds.

2.3 CERSE Project Partners

The organisations listed in Table 1 represent the network of European meteorological and climate institutions that underpin modern weather forecasting and climate research, which are also partners in the CERISE project. This collaboration is essential for addressing the complex, transboundary nature of atmospheric and oceanic phenomena, ensuring consistent, high-quality data and predictive models across the continent.

ECMWF	European Centre for Medium-Range Weather Forecasts
Met Norway	Norwegian Meteorological Institute
SMHI	Swedish Meteorological and Hydrological Institute
MF	Météo-France
DWD	Deutscher Wetterdienst
CMCC	Euro-Mediterranean Center on Climate Change
BSC	Barcelona Supercomputing Centre
DMI	Danish Meteorological Institute
Estellus	Estellus
IPMA	Portuguese Institute for Sea and Atmosphere
NILU	Norwegian Institute for Air Research
MetO	Met Office

Table 1. List of CERISE project partners

3 Skin temperature variable and insights into surface data assimilation

Since understanding and improving the treatment of land–atmosphere interactions is a key step toward developing a more consistent and effective coupled data assimilation (DA) system within CERISE. The two subsections below examine, first, the complexity of handling skin temperature across atmospheric and surface components of the forecasting system, and second, the behaviour of the surface DA system. Together, they provide both conceptual and practical insights that will guide the development of more robust methods for future reanalysis production.

3.1 Skin temperature variable in the atmosphere and the surface forecasting system

One of the ultimate goals of the CERISE project is to design and implement a consistent land–surface–atmosphere DA scheme to enhance the efficient use of satellite-derived data. This is a challenging task because it requires integrating information from systems that were originally developed independently. The realisation of a given quantity in one system can differ from that in another system, as the systems inherently resolve different processes and rely on different assumptions and definitions. This is particularly true for SKT definitions in the upper-air and surface modelling systems.

For the regional reanalysis, the Harmonie-Arome forecasting system is coupled with the ISBA (Interactions between Soil, Biosphere, and Atmosphere) model within the SURFEX (SURFace EXternalisé) platform to simulate energy and water exchanges over natural surfaces. At each time step, the upper-air forecast from the HARMONIE-Arome model provides each surface grid box with so-called atmospheric driving variables, such as upper-air temperature, specific humidity, horizontal wind components, surface pressure, total precipitation, and long- and short-wave direct and diffuse radiation. In return, SURFEX ISBA computes fluxes for momentum, sensible and latent heat, as well as radiative terms such as surface temperature, direct and diffuse radiation, albedo, and surface emissivity.

Although surface temperature is not directly analysed by the upper-air model, it plays a crucial role in extracting information from satellite measurements, as it is a key input to the observation operator that simulates radiances. In the ISBA-Diff model, surface temperature is computed through a soil diffusion scheme and depends on several parameters determined by soil type, such as heat capacity and thermal conductivity. These parameters are difficult to determine at the model grid size due to the strong heterogeneity of soil properties. Complicating matters further, SURFEX operates on four different tiles—nature, town, lake, and sea/ocean. The ISBA-Diff model operates on the “nature” tile, computing fluxes over multiple patches, which in this study correspond to open land. SURFEX then returns the computed information to the upper-air model, averaged over patches and tiles.

A key challenge is that, in the current version of SURFEX, there is no single SKT variable defined across all tiles and patches, even though the upper-air model has a well-defined SKT field. The purpose of the work described in this deliverable is to clarify how skin SKT is treated in SURFEX and the upper-air model, to explore ways of achieving greater consistency in passing SKT information between the two models, and to outline directions for further improvements to fully exploit observations from satellite instruments.

Because of the complexity of the problem, we have decided to explore different directions with the purpose to identify the powerful and still affordable solution to enhance the quality of the new generation reanalysis product.

3.2 Insights into surface data assimilation performance

An experiment was conducted to assimilate 2-metre air temperature and snow thickness observations over the CARRA-NE domain during June–August 2018. The assimilation was performed every three hours using PySurfex with LETKF as the DA scheme. Ten ensemble members were used, and horizontal and vertical localisation radii of 50 km and 200 m, respectively in the LETKF. The analysis focused on the first three ISBA soil layers for temperature estimation, up to eight layers for soil moisture, and twelve layers for the remaining control variables, mainly related to vegetation.

In order to demonstrate a small part of our studies, a point was selected close to the border of Norway and Sweden, see Figure 1a.

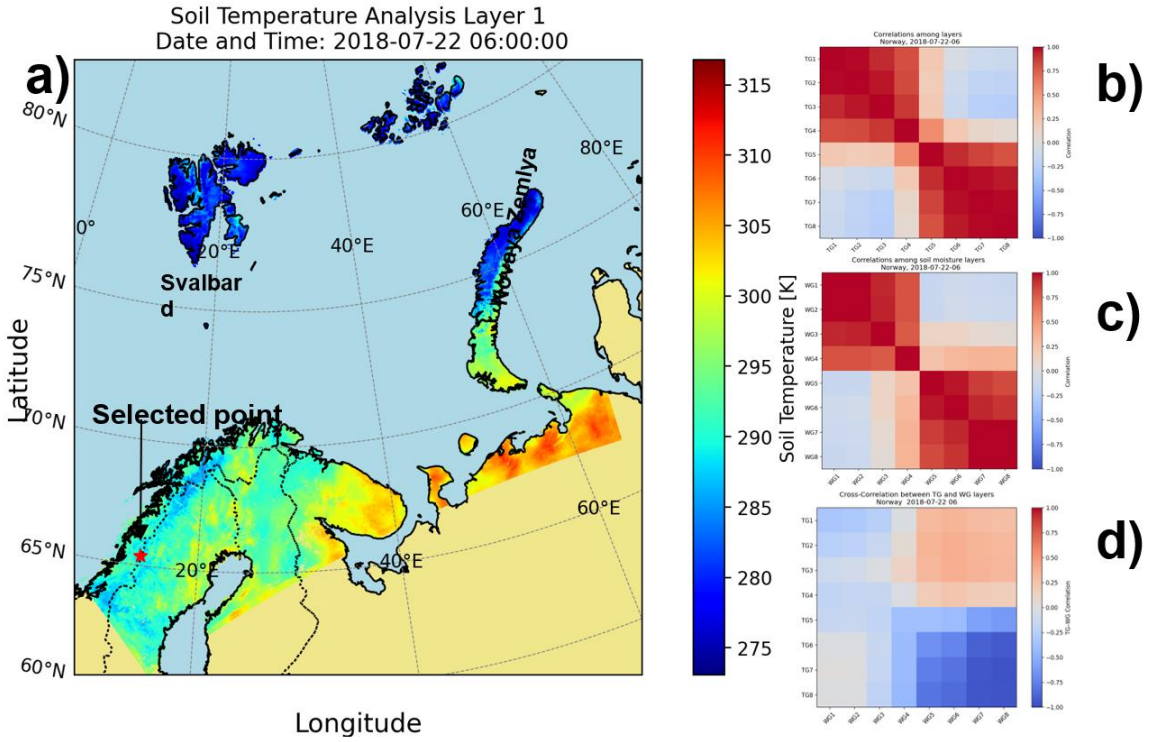

Figure 1. (a) Location of the selected point (red marker) in a steep region on a map of estimated soil temperature at Layer 1. (b) Correlation matrix showing relationships among the ISBA model's soil moisture layers 1 to 8 estimated by the LETKF (Local Ensemble Transform Kalman Filter) in Norway.

Figure 1a displays the soil temperature in Kelvin (K) for the shallowest, the first top layer of ISBA model (Layer 1) used in SURFEX across northern Europe and the Arctic on the 22nd of July 2018 at 6h. It clearly illustrates a sharp thermal boundary: the northern Scandinavian mainland is significantly warm, peaking above 315 K, reflecting strong summer heating in the near-surface soil. In stark contrast, the Arctic islands, Svalbard and Novaya Zemlya, are cold below 285 K, maintaining temperatures characteristic of the active layer in a permafrost regime where cold ground ice suppresses warming, demonstrating a distinct latitude-dependent temperature gradient at the surface.

Figure 1b is a correlation matrix, derived from the ten obtained analysis ensembles, at the selected point in Norway, see Figure 1a, detailing the relationships among soil temperature at eight different layers. It shows two primary groups with distinct, yet internally coherent, behaviours. The shallow layers 1 to 4 are strongly and positively correlated amongst themselves, meaning they tend to wet or dry together in response to surface events like precipitation. Similarly, the deep layers 5 to 8 are also strongly and positively correlated internally. Crucially, there is a clear negative correlation between the shallow and deep group, suggesting that their moisture dynamics are often out of phase. This indicates that short-term wetting in the shallow soil is followed by a time delay before that water drains and impacts the deeper layers, highlighting the complex hydrological processes of infiltration and drainage with depth. Figure 1c is rather similar to Figure 1b and can be explained in the same way. The temperatures in the upper layers are highly correlated and those in the lower layers are also correlated. The correlation between the upper layers (from first to fourth) and lower ones (fifth to eight) are weakly correlated. Figure 1d displays the cross-correlation matrix between eight soil temperature and moisture soil layers. The matrix shows distinct quadrants: the interaction between moisture at the first to fourth layers and temperature of all eight layers indicates a weak or near-zero correlation. However, the fifth to eighth moisture layers reveal a clear split. They correlate strongly and positively with temperature of the upper layers (layers 1-4) and strongly and negatively with those at the lower layers (layers 5-8). This stratified structure demonstrates a significant relationship where the upper and lower temperature layers react in opposite ways to changes in the deeper moisture layers.

It should be noted that the correlation structure and behaviour presented in Figures 1b, 2c and 1d are highly localised to the selected point and the specific time mentioned, as the structure is subject to change spatially and temporally and can highly change.

4 Weakly coupled data assimilation of AMSR2 brightness temperature

This section focuses on the weakly coupled assimilation of satellite brightness temperature observations to constrain land surface variables, with a particular emphasis on soil temperature over non-frozen land. It introduces the data and methods used, including the HARMONIE-AROME forecasting system, AMSR2 satellite observations, and a machine learning-based observation operator. Key adaptations to the data assimilation (DA) framework, such as modifications to the LETKF, observation selection strategies, and an adaptive observation error scheme, are also described. Together, these subsections provide a detailed overview of the implementation, rationale, and performance considerations for integrating satellite data into a coupled land–atmosphere assimilation system.

4.1 Background

The focus here is on the coupled assimilation of satellite radiances to constrain land surface variables. These radiances can be utilised to constrain quantities e.g. snow heat, soil temperature and moisture, and snow-on-sea-ice heat content. In this study, we focus on soil temperature over non-frozen land, as it has the most direct relationship with the satellite observations; see Fig. 2. The unified land DA system developed in WP1, reported in D1.3, and the machine learning observation operator from T1.4, reported in D1.4, are applied to assimilate AMSR-2 brightness temperatures. Other land surface variables, such as soil moisture and snow, remain in the control vector, but the primary focus is on the impact on soil temperature. The unified land DA system is coupled to the HARMONIE-AROME NWP model, forming a weakly coupled land–atmosphere DA system, where the LETKF updates surface variables and 3D-VAR updates the atmosphere. Coupling between the two interfaces occurs at each three-hour forecast step between assimilation cycles.

4.2 Data and methods

This section outlines the HARMONIE-AROME model configuration, the satellite observations from AMSR2, and the machine learning-based observation operator used to relate satellite brightness temperatures to land surface variables. Key aspects of the assimilation system are detailed, including the selection and treatment of observations, modifications to the LETKF to handle large numbers of observations, and the use of an adaptive observation error scheme to improve assimilation quality. Together, these methods provide the framework for evaluating the impact of satellite data on soil temperature and other land surface variables.

4.2.1 HARMONIE-AROME model

The HARMONIE-AROME configuration is the same as used in the CARRA2 re-analysis. CARRA2 runs 3D-VAR for the atmospheric DA and the simplified extended Kalman filter (SEKF) for the surface soil DA. This latter is here replaced by the LETKF. We made a few modifications to the system to be able to run on a smaller domain covering the Nordic countries.

4.2.2 Satellite data

In our analysis we use observations from the AMSR2 sensor. This instrument sits onboard the GCOM-W1 Japan Aerospace Exploration Agency (JAXA) satellite. It measures passive microwaves in vertical and horizontal polarization at the following frequencies: 6.925, 7.3, 10.65, 18.7, 23.8, 36.5 and 89.0 GHz. The satellite swath width is 1450 km with an incidence angle of 55°. It follows a polar orbit with overpasses at 1:30 am and 1:30 pm local time. In our study we focus on the 18GHz channel. We use level 1 data from JAXA, it contains swath data with locations and spatial resolution ranging from ~7 to ~40 km depending on frequency.

4.2.3 Observation operator

In T1.4 we developed a machine learning observation operator based on graph neural networks (GNN). In the GNN observation operator each graph has a set of nodes. Each node corresponds to an AMSR2 observation. Within the footprint area each node has a selected number of features, e.g. the ISBA land surface variables grid-points. The area of the footprint is frequency dependent, thus is also the number of features for each frequency. We utilize a static number of grid cells for each individual frequency, hence the GNN is said to be a static-GNN. We also tested a GNN where the number of nodes within the swath was allowed to vary. This is because the observations at the edge of a swath have a larger footprint than the observations close to the center, hence the number of ISBA grid-cells within a footprint is larger at the edge than at the center of the swath. This dynamic (varying nodes) was tested and found to give better results than the static-GNN (not shown). The computational cost of training the static-GNN was lower than for the dynamic-GNN and summary scores did not suffer too much of keeping the number of nodes static.

4.2.4 Brightness temperature assimilation

Low frequency passive microwave observations are sensitive to both soil moisture and temperature (Kerr et al., 2010, Entekhabi et al., 2014). An example of the correlation between soil temperature in layer 1 (1 cm) with AMSR2 brightness temperature observations (18GHz V and H-pol) is given in Fig 3.1, for JJA 2018. The rationale for choosing the 18GHz channel is therefore i) it has a high correlation with surface soil temperature; and ii) with respect to the observation operator, the 18GHz channel has medium complexity. With complexity we here mean the number of ISBA grid-cells used for each node in the observation, 80 for 10GHz, 25 for 18GHz and 5 for 36GHz. So even though we expect the 10GHz channel to have more sensitivity to land surface variables we opted for the 18GHz channel as these are initial tests for applying the observation operator and the LETKF in a weakly coupled DA system.

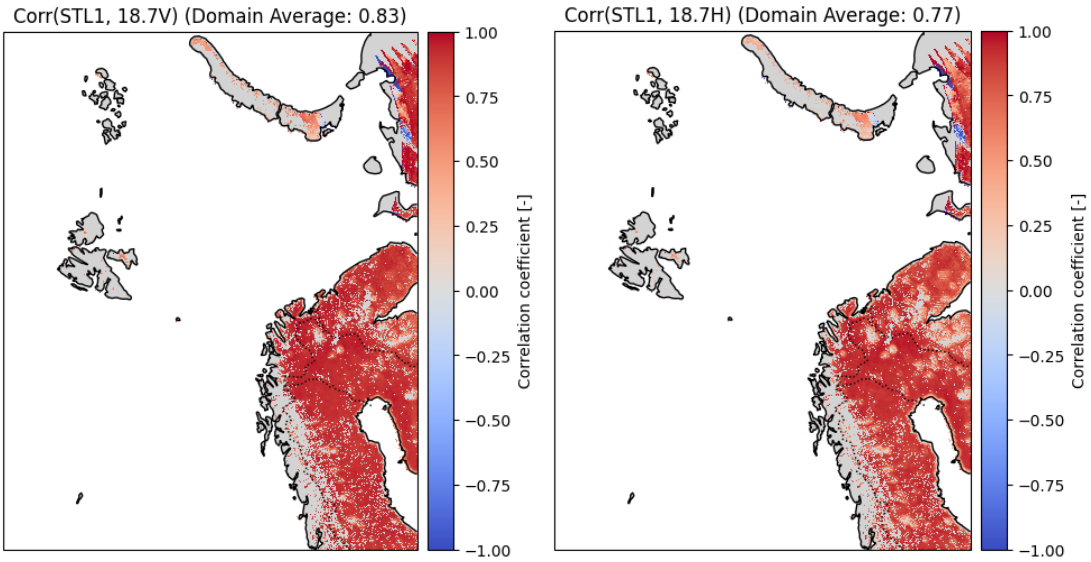

Figure 3.1: Temporal correlation between soil temperature layer 1 (1 cm) and AMSR2 18GHz V and H-pol brightness temperature for June, July and August 2018.

4.2.5 Adaptions to the LETKF

Introducing satellite observations requires the DA system to handle a large number of observations. Furthermore, in situ and satellite observations need to be treated differently in terms of localization and representative area. To allow some flexibility in this regard, we have modified the DA system relative to the CARRA-Land-Pv1. For each observation type it is possible to specify the observation error, horizontal and vertical impact radii and the number of observations to be used per grid point. In the LETKF, all observations could in theory be used, but reducing the number is reasonable both with respect to computational and meteorological performance. The maximum number of observations per grid point is set per observation type so that less dense observations like in situ are still used where very dense observations, for example from satellites, are present.

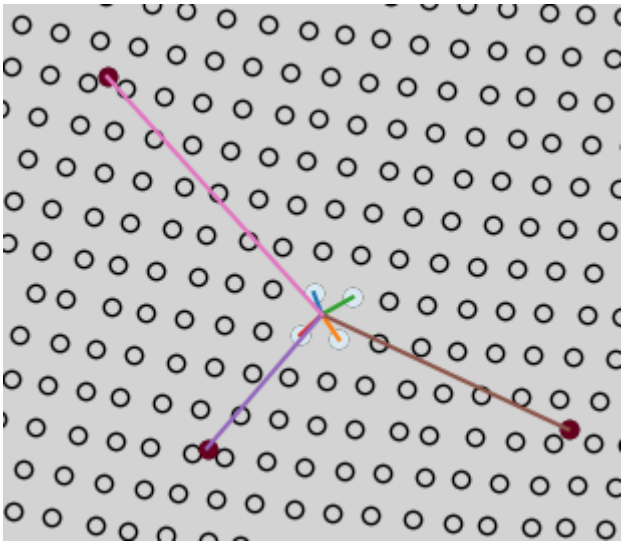

Figure 3.2: Illustration of observation selection, three in situ stations (red) and four AMSR2 Tb observations (white) are selected.

This observation selection strategy is illustrated in Fig. 3.2, here we see that the model grid-cell uses 4 AMSR2 footprints (white circles) and 3 in situ observations. In our experiments we set the number of in situ and satellite observations to 6 and 1, respectively.

4.2.6 Adaptive observation error in the LETKF

Introducing satellite brightness temperature observations requires different quality control schemes compared to in situ observations. In this work we use a two-step approach. i) A first guess check that removes observations where observation minus first guess (O-F) are greater than a constant (e.g., 5) times the prescribed observation error; ii) an adaptive observation error scheme following Sakov & Sandery (2017) [https://doi.org/10.1080/16000870.2017.1318031)], where the observation error is adjusted as a function of O-F. The function is constructed such that for zero O-F the observation error is the prescribed value and that for large O-F, the maximum increment is the first guess error standard deviation times a constant (e.g., 2). The behaviour of this adaptive observation error is illustrated in Fig. 3.3. In the left figure we see the observation errors and in the right figure we see the O-F used to calculate the observation error. We see that for regions where the O-F is large the original observation error (5 K) is inflated to larger values, e.g., 8-9 K.

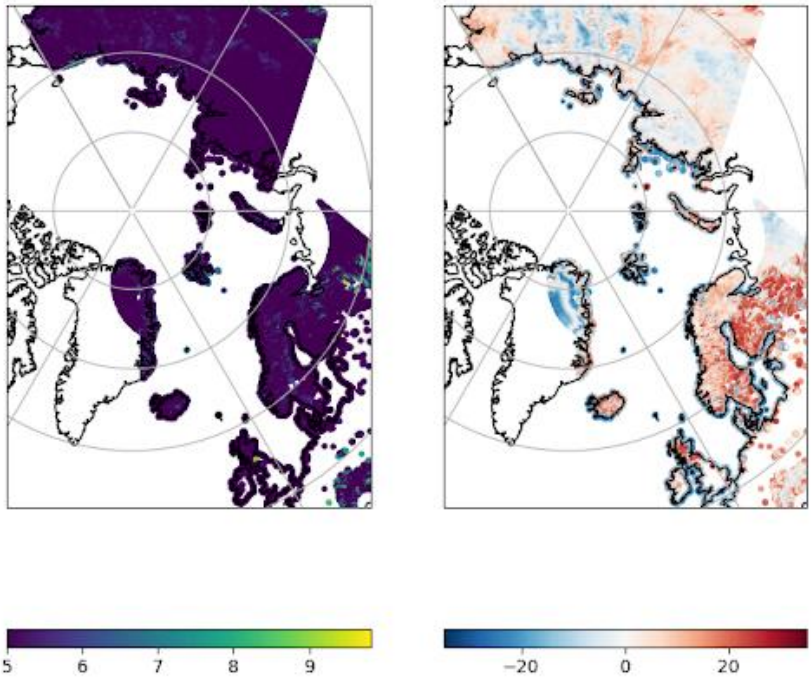

Figure 3.3: Example of adaptive observation error. AMSR2 18.7V 00h-03h overpasses, left panel shows adaptive observation errors (Kelvin) and right shows O-F (Kelvin).

4.3 Experimental setup

We set up two different experiments to evaluate the assimilation of AMSR2 observations in the weakly coupled DA system. The baseline experiment assimilates 2m temperature synop observations and updates soil temperature and moisture. The AMSR2 experiment utilizes the same observations as the reference, but in addition we assimilate 18GHz V-pol AMSR2 observations at 03UTC. The 03UTC overpass was selected because we assume that the land-atmosphere is closer to thermal equilibrium during night-time than mid-day. The observation error for 2m temperature is set to 2 K and the horizontal and vertical influence radius are set to 30 km and 200 m, respectively. For 2m temperature we allow 6 in situ stations to influence one grid-cell, given that they are inside the horizontal localization radius. For AMSR2 observations the observation error is set to 5 K, horizontal radius to 9 km and 1 AMSR2 observation is allowed to influence a given grid-cell. Our experiments start on the 1st August 2025 and run until 26th August 2025. The first seven days are taken as spin-up and are left out of the verification.

4.4 Results

In this section we present data assimilation diagnostics Sect. 3.3.1, screen level and atmospheric verification Sect. 3.3.2 and finally soil verification in Sect. 3.3.3.

4.4.1 Data assimilation diagnostics

The unified land data assimilation system has been evaluated in D1.3 and in D4.3. Here we briefly show some data assimilation diagnostics to illustrate the difference when adding AMSR2 observations in the assimilation. Figure 3.4, shows instantaneous increments (Analysis-minus-Firstguess) for soil temperature (top 4 cm of soil) top and soil moisture (top 10 cm of soil) bottom. For 2m temperature only (left) and 2m temperature + AMSR2 assimilation (right). The increments are for 25th August 2025 03 UTC. For in situ only (left) we

see that the increments are mostly concentrated around the observation points. We also note that for most of the increments, an increase in temperature is followed by a decrease in soil moisture. For in situ + AMSR2 (right) we still see the SYNOP stations in the increments, but in addition we see the effect of having AMSR2 observations (covering the whole domain during 00 to 03 UTC). For soil moisture we note that there is a coastal effect in the increments (bottom right). This is likely because of the AMSR2 footprint covering both land and sea, while the ISBA grid-cell is still 100% land. To remove this, we would need further masking of observations based on distance from water rather than land surface model characteristics only. Another option is to include e.g. sea surface temperature in the inputs to the observation operator, it could then most likely improve the predictions for mixed land-sea pixels. For smaller inland waters/lakes this problem is most likely avoided because for the satellite footprint there will be some ISBA LSVs in the graph that can be used to explain the variability of the brightness temperature. Here we could further improve the observation operator by adding e.g. lake skin temperature.

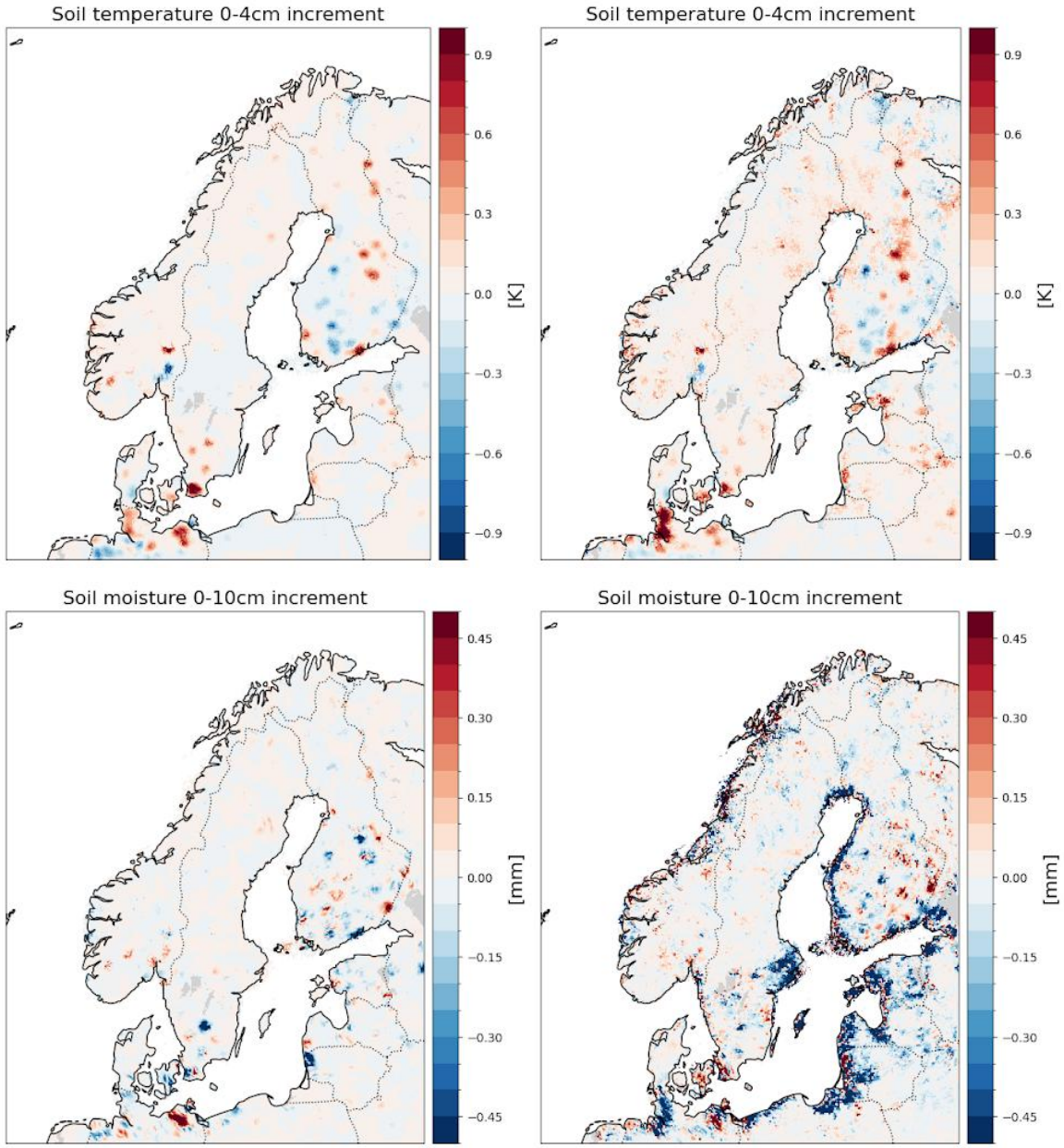

Figure 3.4: Top left, instantaneous soil temperature increment for CARRA3-Pv1_insitu and, top right, the same but with AMSR2 assimilation, both are for 25-08-2025 03 UTC top 4 cm of the soil. Bottom left, soil moisture instantaneous increment (mm) for CARRA3-Pv1_insitu top 10 cm of soil and, bottom right, the same but with AMSR2 assimilation.

To evaluate the typical size of the increments we plot the temporal standard deviation of the ensemble standard deviation of increments, see Fig. 3.5. Left shows for CARRA3-Pv1_insitu and right shows for CARRA3-Pv1_AMSR2. In the former we clearly see that the increments during this time-period are very localized (bull's eye) and that the horizontal influence radius for 2m temperature most likely could be increased. In the latter we see that there are more increments throughout the domain because of the AMSR2 observations, but that these increments are smaller than for the 2m temperature observations. This is due to the larger observation error for the AMSR2 observations.

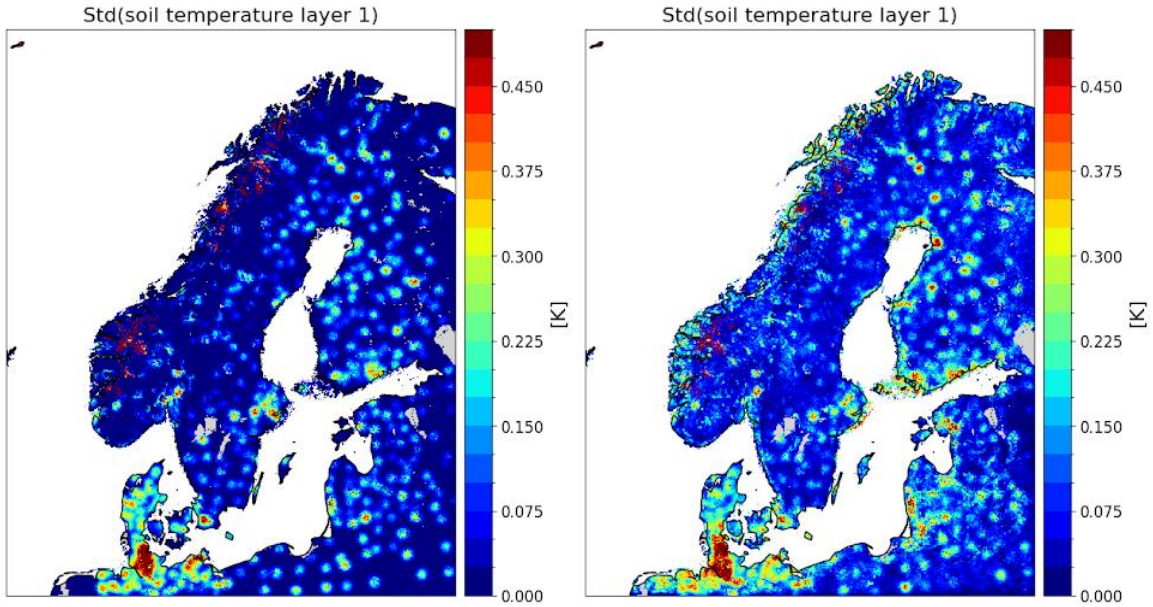

Figure 3.5: (Left) Soil temperature layer 1 standard deviation in time of ensemble standard deviation for CARRA3-Pv1_insitu (2m temperature and humidity assimilation). (Right) same but in addition assimilation of AMSR2 data. Time period 2025-08-07 to 2025-08-26 03 UTC.

4.4.2 Screen level and atmosphere verification

To evaluate the weakly coupled data assimilation system and the influence of AMSR2 assimilation on the coupled system, we look into screen level 2m temperature and relative humidity verification and also into temperature and specific humidity profiles verification against radiosondes. Figure 3.6 (top) shows the bias between observation and 2m temperature averaged over all stations throughout the experiment time period. The orange line is the CARRA3-Pv1_insitu and the blue line is the CARRA3-Pv1_AMSR2 experiment. There are small differences in the bias; we see that the CARRA3-Pv1_AMSR2 experiment has somewhat less cold bias for the cold bias "peaks". Figure 3.6 (bottom) shows the same but for mean-absolute-error (MAE). Here the difference between the two experiments is very small.

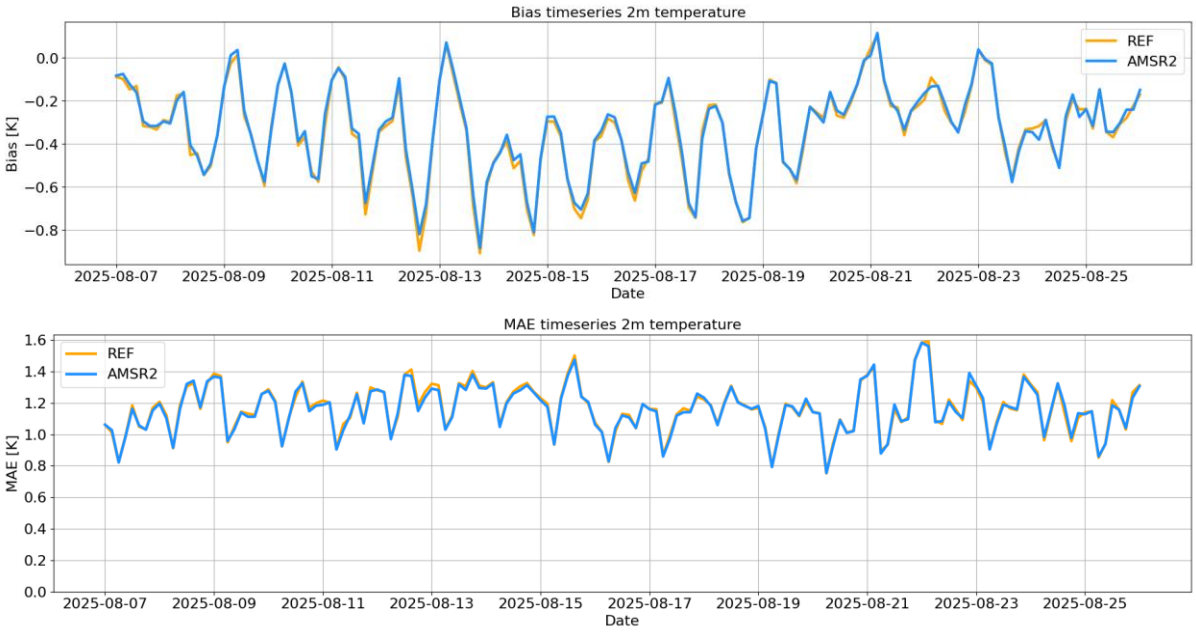

Figure 3.6: (Top) 2m temperature bias time series for REF (synop 2m temperature assimilation only) and AMSR2 (2m temperature + AMSR2 observations assimilated). (Bottom) same but for mean-absolute-error. Time-period is 2025-08-07 00UTC to 2025-08-26 00UTC.

Statistics for relative humidity are shown in Fig. 3.7. For the bias (top) we see that the CARRA3-Pv1_AMSR2 experiment has less wet bias during the peaks (noting that the difference is very minor). The same is seen for the MAE which is somewhat smaller during the peak errors.

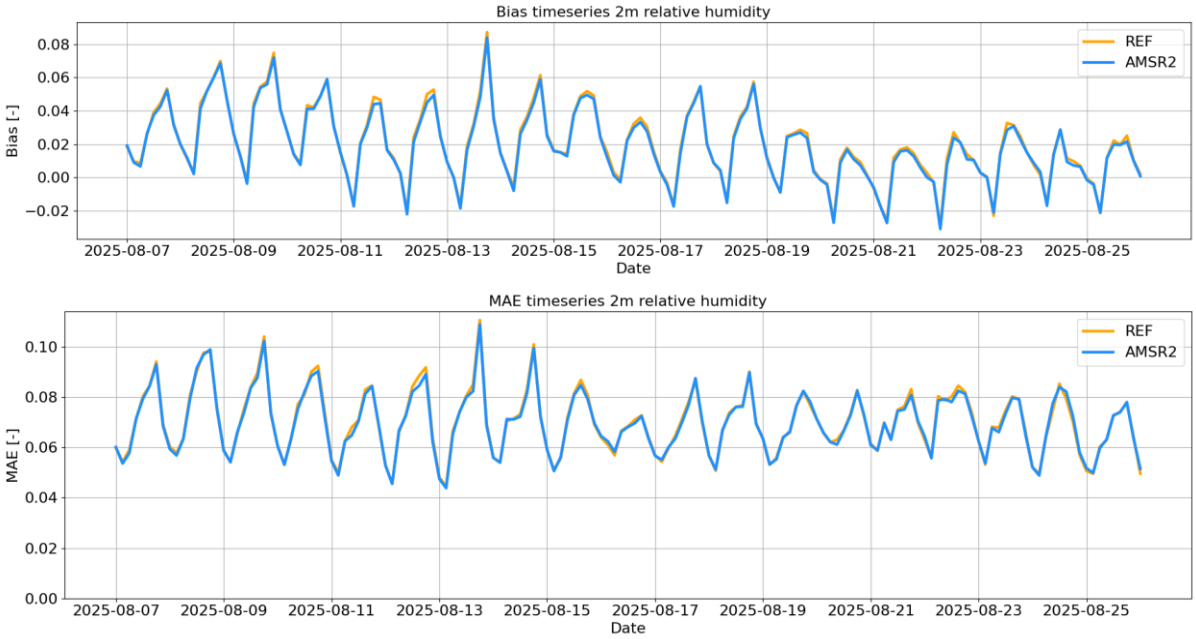

Figure 3.7: (Top) 2m relative humidity bias timeseries for REF (synop 2m temperature and humidity assimilation only) and AMSR2 (Synop + AMSR2 observations assimilated). (Bottom) same but for mean-absolute-error. Time-period is 2025-08-07 00UTC to 2025-08-26 00UTC.

To evaluate how the surface assimilation affects the atmosphere we plot verification of temperature and specific humidity versus radiosonde observation. There are in total 16 radiosonde stations within the domain, which we average over time and over all stations.

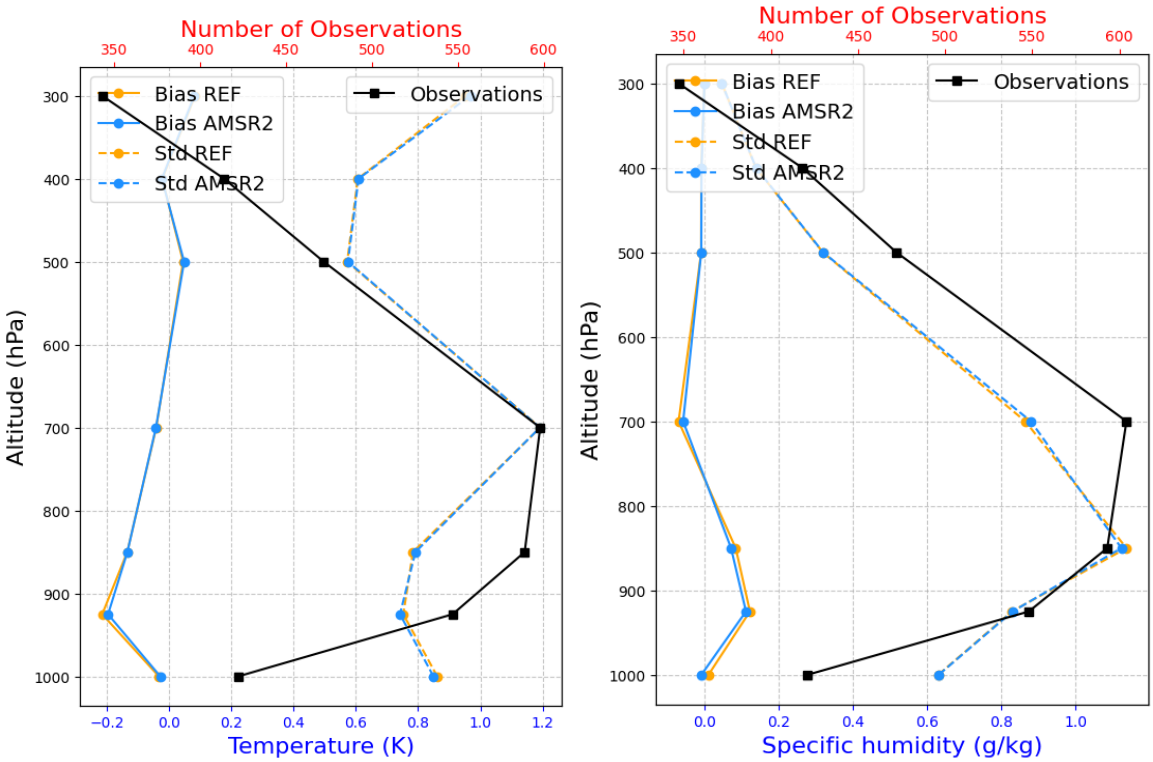

Figure 3.8: Bias and std of errors for temperature (left) and specific humidity (right). Bias in solid line and std in dotted line. The number of observations for each altitude is plotted in black. Average over 16 stations for the time-period 2025-08-07 00UTC to 2025-08-26 00UTC.

Vertical profile of bias and std of errors are shown in Fig. 3.8 (left) for temperature and (right) for specific humidity. Again, the differences are minor, but we see that the CARRA3-Pv1_AMSR2 experiment has somewhat lower std of temperature errors (dotted blue line vs dotted orange) and less bias for the specific humidity (solid blue line vs orange).

4.4.3 Soil verification

The impact on soil variables is evaluated using in situ observations of soil moisture and soil temperature. The number of stations observing these variables are very limited within our domain and we focus on observations from the Finnish Meteorological Institute Sodankyle station. Figure 3.9, shows soil moisture time series for three different stations close to Sodankyle (station id: SO011, SOD130 and SOD140). Note that CARRA3-Pv1_AMSR2 (blue) and CARRA3-Pv1_insitu (orange) do not start at the same soil moisture value on 7th of August 2025, because of the 7-day spinup. One thing to note is that the CARRA3-Pv1_AMSR2 experiment seems to dampen some of the peaks, e.g., see SOD011 around 11th and 12th of August.

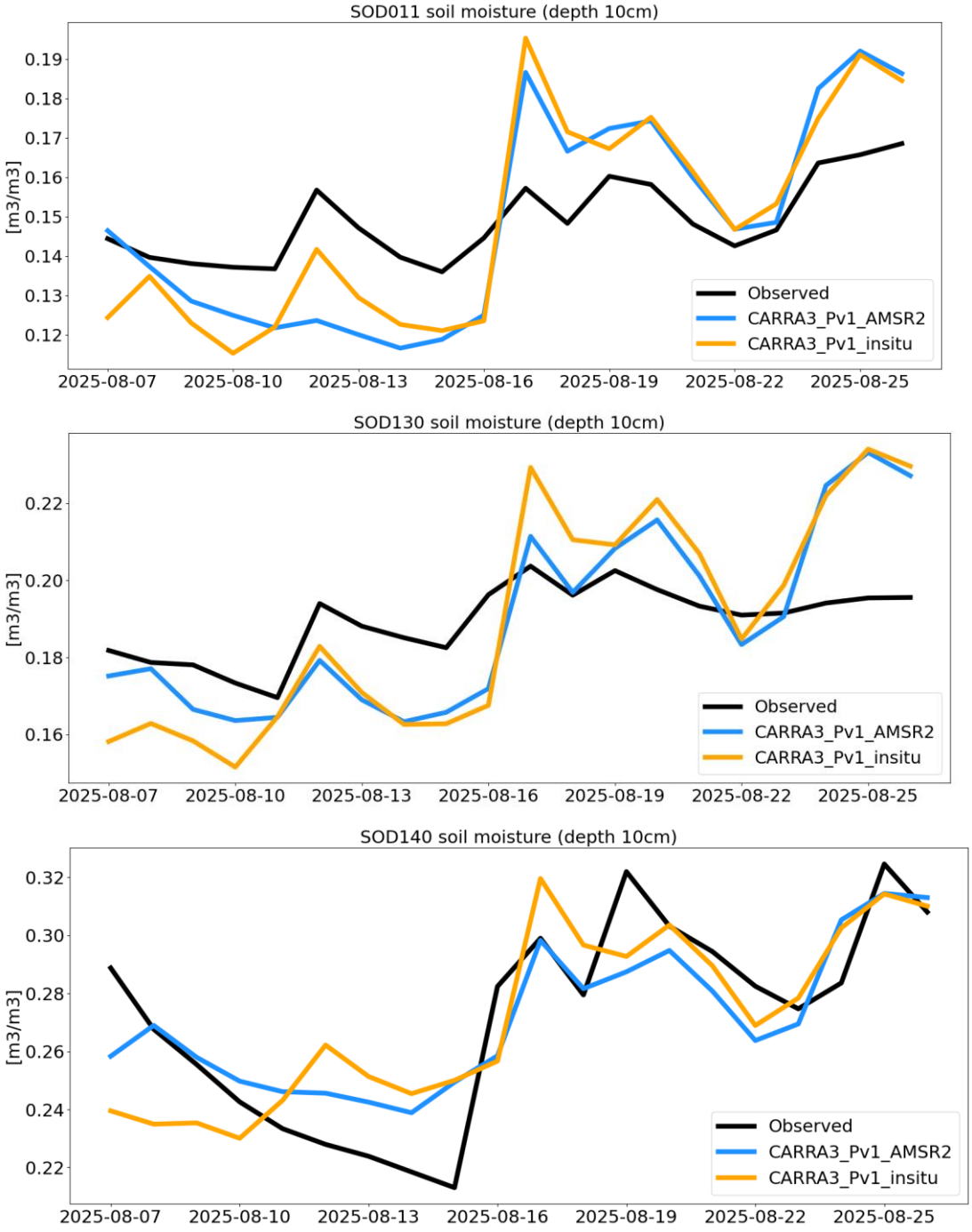

Figure 3.9: (Top) Soil moisture time-series from FMI station id SOD011 (67.36N, 26.63E), observations (black), CARRA3-Pv1_AMSR (blue) and CARRA3-Pv1_insitu (orange). Daily average from 2025-08-07 to 2025-08-26. For ease of comparison the mean simulated bias was removed from the time-series prior to plotting. Middle and bottom, same as top but for station id SOD130 (67.26N, 26.75E) and SOD140 (67.15N, 26.73E).

We compute the anomaly correlation coefficient (ACC) between observed and simulated soil moisture, see Tab. 3.1. Here we see that the CARRA3-Pv1_insitu experiment has a higher ACC than the CARRA3-Pv1_AMSR2 in 2/3 stations.

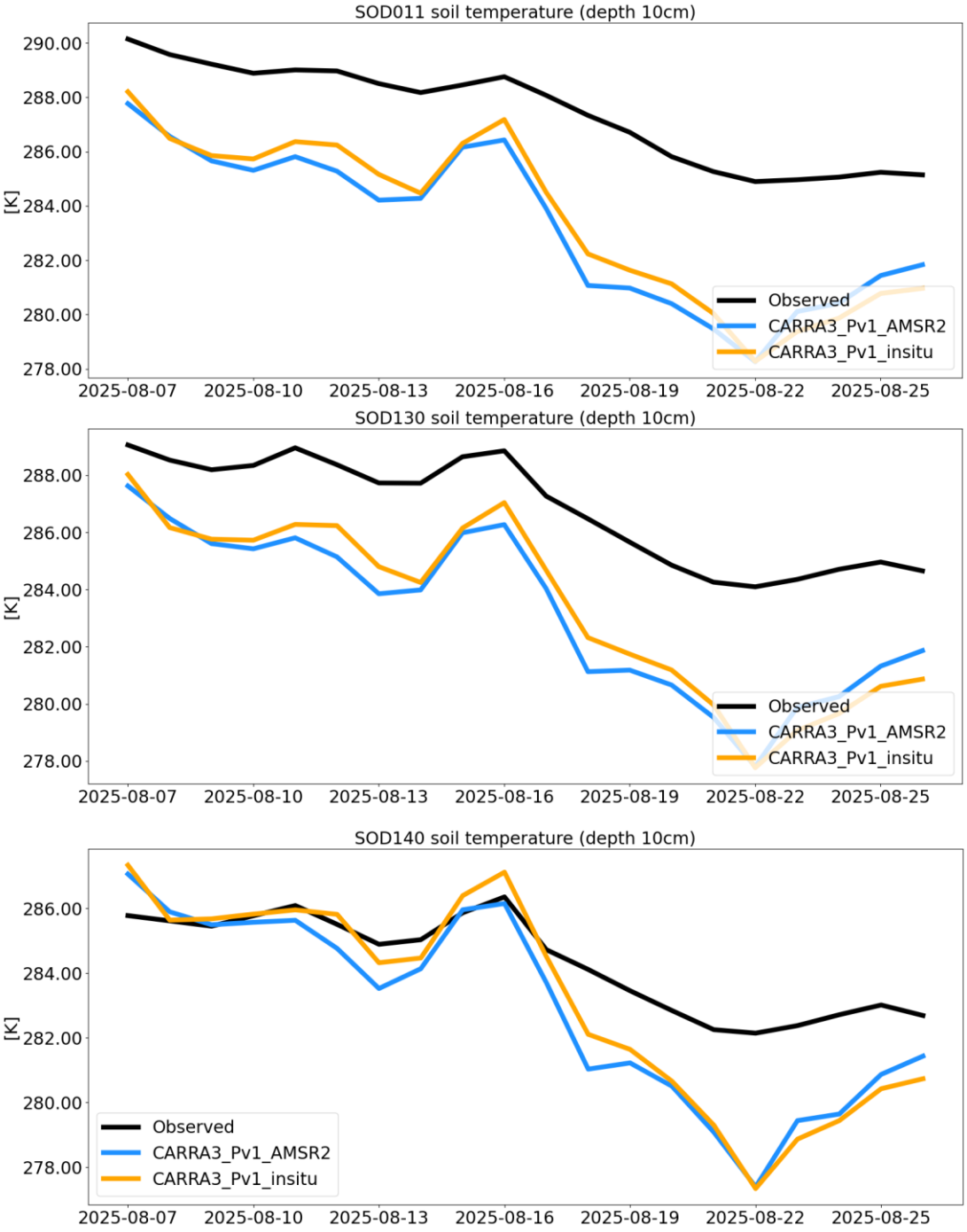

Figure 3.10: (Top) Soil temperature time-series from FMI station id SOD011 (67.36N, 26.63E), observations (black), CARRA3-Pv1_AMSR (blue) and CARRA3-Pv1_insitu (orange). Daily average from 2025-08-07 to 2025-08-26. Middle and bottom, same as top but for station id SOD130 (67.26N, 26.75E) and SOD140 (67.15N, 26.73E).

Soil temperature is plotted for the same stations as moisture in Fig. 3.10. Here we see that there is some bias between the simulated and observed temperature. The ACC is high for temperature and the CARRA3-Pv1_insitu experiments have the highest skill, see Tab. 3.1.

Table 3.1: Anomaly correlation coefficient for soil moisture and temperature for three different in situ stations.

	SOD011		SOD130		SOD140	
Experiment	**REF**	**AMSR2**	**REF**	**AMSR2**	**REF**	**AMSR2**
Soil moisture	**0.86**	0.83	**0.80**	0.73	0.73	**0.86**
Soil temperature	**0.97**	0.94	**0.98**	0.96	**0.98**	0.97

5 5. Outer-loop 4DVAR land surface atmosphere coupling

5.1 Background.

In this section we focus on the ability of the outer-loop HARMONIE-Arome 4D-Variational data assimilation scheme (Barkmeijer et al, 2021) to communicate surface temperature information between the upper-air and surface models. The idea of 4DVAR is to use the latest available observations collected over an assimilation window to sequentially improve the initial state for the forecast model. The initial state is determined by minimizing the cost-function that consists of two terms, the first one measuring the distance of the 3D-initial state to the background (a short-term forecast) and the second one measuring the distance from the model trajectory issued from the initial state to the observations distributed over data assimilation window. In other words, 4DVAR uses the forecast model evolution as a strong constraint. Because of the non-linearity of the forecast evolution the incremental 4DVAR has been proposed where the initial state is computed iteratively through the so-called outer-loop approach. During each outer-loop the forecast model equations are linearized around the model trajectory run, and the initial state is computed for the linearized model. The obtained initial state is used to improve the model trajectory for the next outer loop, and the initial state is re-estimated. When forecast models for different Earth-system components are integrated in a coupled way, by interacting with each other during every time step, the outer-loop 4DVar provides a framework for coupled data assimilation, in this case atmosphere and land. This approach relies on the information exchange during the same assimilation window between the domains when producing the analysis which is separate between components. The communication between Earth-system components happens when computing the trajectory, which is basically a coupled forward forecast model along the assimilation window, when the land surface and the atmosphere exchange the information each time step.

5.2 Configuration of the Harmonie-Arome outer-loop 4DVAR

Figure 4.1 depicts the different blocks for the experiment configuration, where it can be seen that inside each outer loop a surface analysis block is placed. This land assimilation scheme is based on the SEKF technique implemented in the SURFEX platform for nature tile. The SEKF assimilates screen-level temperature, relative humidity and snow depth fields obtained through optimal-interpolation from quality-controlled observations. The SEKF propagates the two-meter increments into deep soil levels for each grid-point separately. The propagation is based on the blocks marked in red as “Offline surfex”, responsible for computing the Jacobians by applying perturbations. The offline ISBA-DIF model is used to evolve perturbed surface model states forced by atmospheric forcing fields. It is important to note that land assimilation is carried out at the beginning of the 4DVar assimilation window.

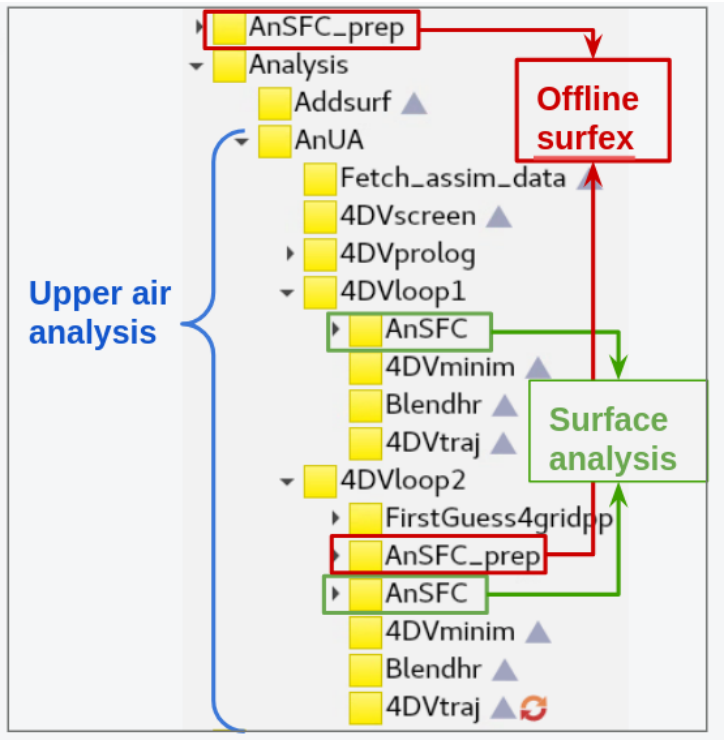

Figure 4.1. Experiment configuration for outer loop coupling

5.3 The exchange of information between the atmosphere and the land model components

The exchange of information within the assimilation window between the land and atmosphere components is now described. Coupling from land to atmospheric fields is a consequence of the aforementioned trajectory runs. The 4DVar minimization during the first loop is not affected by the land data assimilation performed in the same loop. However, the trajectory run in the first outer-loop is initiated from the land and the atmospheric analysis at the beginning of the assimilation window. This trajectory run updates the analysis departures from low- to high-resolution fields, being also influenced by the integration of the coupled model. The resulting analysis departures are used to update the background state in the next outer loop's minimization. Similarly, the land analysis within the second loop is set as the initial field for the corresponding trajectory run. In this case, the trajectory run, with the coupled model integration, is used to obtain the forecast initial state, defined here at two hours from the beginning of the assimilation window.

On the other hand, the coupling from upper air to the soil is the result of two different paths. The first one is the re-diagnosis of the screen-level fields (two-meter fields) with the updated upper-air fields during the trajectory run. These updated fields are used as background state during the subsequent assimilation (optimal interpolation). The second path is by updating the Jacobian of the observation operator used in the second loop along the trajectory run from the first outer loop, instead of the already computed Jacobian from the previous cycle forecast.

5.4 The analysis of the outer-loop 4DVAR performance

To study the stability of the configuration, the experiment has been run for two weeks. Figure 4.2 shows 2 metrics of interest in this regard. The top plot shows the total cost function, i.e.,

the sum of background and observation distance contributions, for the cycles under study for both outer loops. It can be seen that within each cycle and outer loop, the total cost is reduced. Some cycles show a higher cost, appearing at a regular interval. These cycles correspond to 0 and 12 UTC, where numerous radiosonde observations are available. The gradient norm evolution with cycles is depicted in the bottom plot, where the reduction at each cycle and loop is also noticeable. Finally, the observation cost function contribution at the end of the minimization is presented in figure 4.3 for some selected observations. This quantity is normalized by the number of observations, where values below 1 are generally used as a sanity check, as is the general trend here.

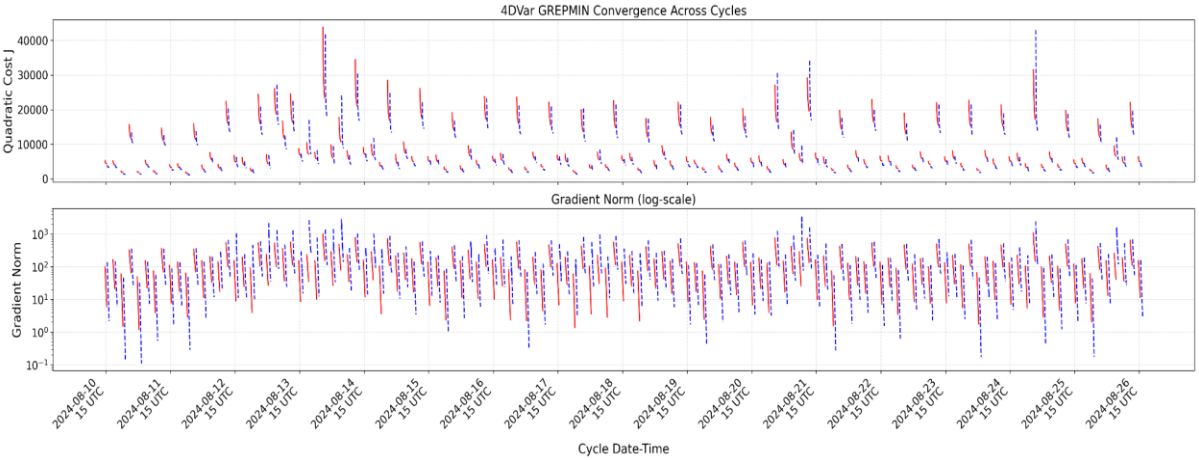

Figure 4.2. (Top) Total cost function for the cycles under study for both outer loops. (Bottom) Gradient norm during minimization.

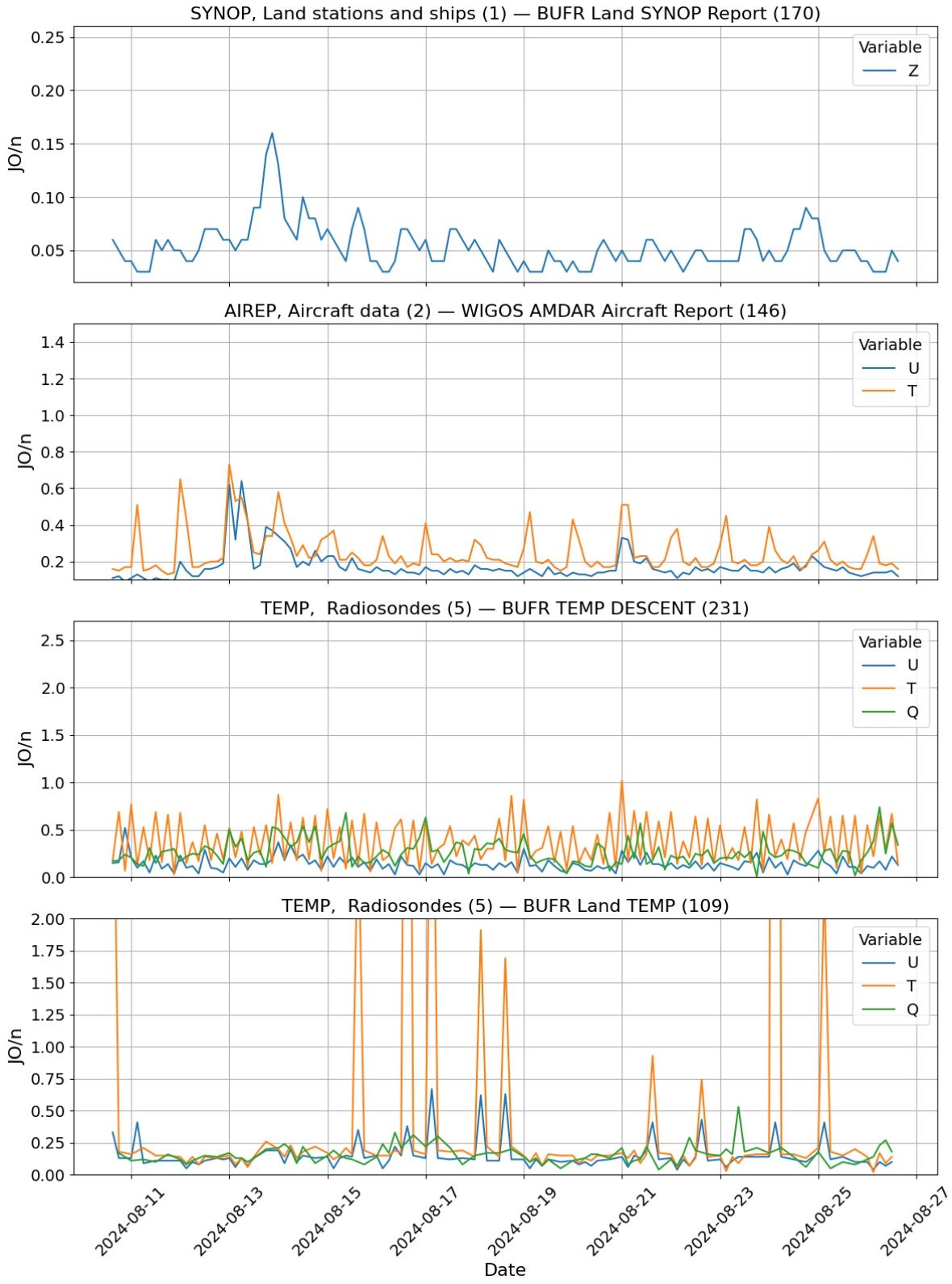

Figure 4.3. Cost function contribution for selected observation normalized by the corresponding number of observations.

Except for a few cycles, the three metrics discussed above show that the experiment is rather stable in its current form. However, a few points should be highlighted due to their possible impact on the ability of the 4DVAR outer-loop to pass information between land and

atmosphere components. It can be seen in the total cost function plot that for some cycles, the second outer loop starts at a higher value than the first one. This indicates that the fit to the observations of the first-guess state in the beginning of the second outer-loop is worse than in the beginning of the first outer-loop. At the same time the analysis from the second outer loop comes closer to observations than the analysis from the first outer-loop. In most cases the gradient norm of the end of the second outer-loop is lower than the gradient norm at the end of the first outer-loop indicating the healthy behaviour of the system. Figure 4.4 shows the contribution to the cost function from each observation type at the first minimization iteration of each outer loop for a cycle presenting this behaviour (2024-08-25 00 UTC). It can be seen that the wind measured by BUFR Land Temp is the driver of the higher cost function value. It should be noted that the first-guess of this specific cycle is initiated at 2024-08-24 21 UTC when the number of observations is extremely low and dominated by surface observations, indicating a biased wind field. The increase in the cost function during the second outer-loop seems to be related to the next point to be highlighted, which is the peaks in the temperature and wind observations shown in the bottom plot of figure 4.3 for radiosondes as well. Those high peaks occur at cycles 03 and 15 UTC, after the cycles with a large number of radiosonde observations at 00 and 12 UTC. In particular, the last peak in the plot corresponds to the cycle 2025-08-25 03 UTC. The second outer loop at the 2025-08-25 00 UTC has managed to fit wind observations closely, but the forecast from it, the first-guess for the 2025-08-25 03 UTC, seems to result in a biased temperature field, degrading the quality of the temperature forecasts. It is still unclear to what extent the exchange of the information between land and surface components contribute to the problem. Is there a conceptual issue with the exchange of the information between land surface and atmosphere in the HARMONIE forecasting system when the large-scale systematic biases affect components? Or are there deficiencies in the implementation? Further work is required to address these questions.

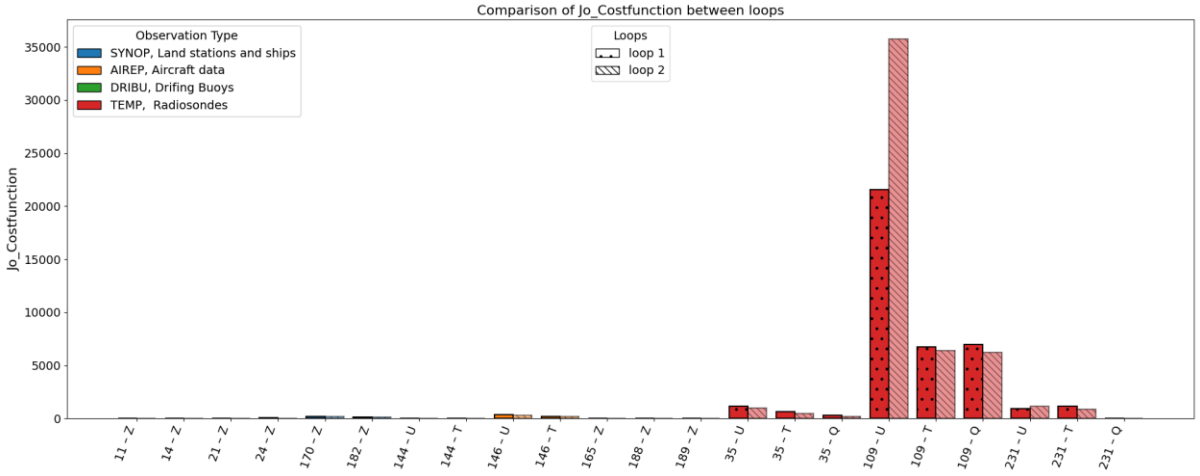

Figure 4.4. Contribution to the total cost-function during the first minimization iteration for the first and the second outer loop by observation types at 2025-08-25 00 UTC.

6 Extended Control Variable Approach

6.1 Background

One of the implemented schemes is based on the extended control vector approach for the upper air data assimilation following the implementation described in (Gustafsson el al, 2014). The extended control vector approach is an extension of the variational data assimilation scheme described in Section 4.1. As it is explained above the variational cost function for minimization consists of two terms, one of which measures the distance of the analysis to the background. This distance is measured using the forecast error covariance term. In a standard formulation the climatological forecast error covariance estimate is used. The measure works well on average but might be misrepresenting in particular situations. The climatological forecast error covariance is derived based on restricting assumptions that are not fully valid for convective scale motions (Bojarova and Gustafsson, 2019). The extended control vector approach allows to integrate forecast error-of-the-day statistics by utilizing the forecast-error statistics derived from the ensemble evolution. Each ensemble member is integrated by the coupled forward atmosphere land surface model, when the HARMONIE-Arome atmosphere model and the land surface ISBA-Dif model exchange the information each time step. This methodology allows to obtain an analysis correction to the skin temperature consistent with the upper air data assimilation and pass it to the surface data assimilation scheme. As a result, tiny balances and dependencies are built between all model components. As it is mentioned above in Section 3 in the SURFEX platform there is no skin temperature variable consistently defined over various tiles and patches. In the current implementation we have decided to use the “skin-temperature” variable stored as temperature at the upper most soil level and accessed through its “gribcode” NGRBSTL1 (139) and abbreviated as “SURFTEMPERATURE”.

6.2 Implementation

In order to obtain an analysis increment of skin temperature, we augment the control variable (χ) with a set of the two-dimensional fields representing ensemble weights (α). The forecast error covariance is represented by its climatological part (B) and the error-of-the-day part derived from the ensemble of perturbations ($x=X-X^b$) and is used to project the control vector to the physical space. In the current implementation we have used the perturbation around control (X^b), namely the perturbation is obtained by substructing the evolution of the control member from each ensemble member. The perturbation around the mean evolution is a possible alternative, but it does not guarantee that the perturbation obtained in this way is physically consistent. The error-of-the-day part contains both the upper air standard dynamical variables such as mass, wind and moisture on model levels (x_{vor}, x_{div}, $x_{tem/ps}$, x_{hum}) and the extended variables, the skin temperature (x_{ts}) in our case. The ensemble weights are obtained by solving the variational upper air data assimilation problem where the analysis increment is computed as a sum of the contributions from the climatological error structures (abbreviated Δx_{var}) and the error-of-the-day ensemble structures (Δx_{ens}). As a remedy of the limited ensemble size, the covariance localisation has to be applied (A). In this scheme we have chosen to apply the space-scale dependent localisation to be able to efficiently treat processes on different scales (Buehner and Shlyaeva, 2015). The ensemble of forecast states is decomposed into the i overlapping spectral bands and different localisation scales (A_i). This allows to apply a flexible localisation length dependent on the spatial variability of the field preserving heterogeneity of the forecast error structure. When the optimal weights are obtained as a result of the minimization of cost function, the analysis increment of the extended surface temperature variable can be computed from the ensemble of forecast states. The

surface temperature analysis increment is passed to the SEKF scheme to update soil variables on deeper levels.

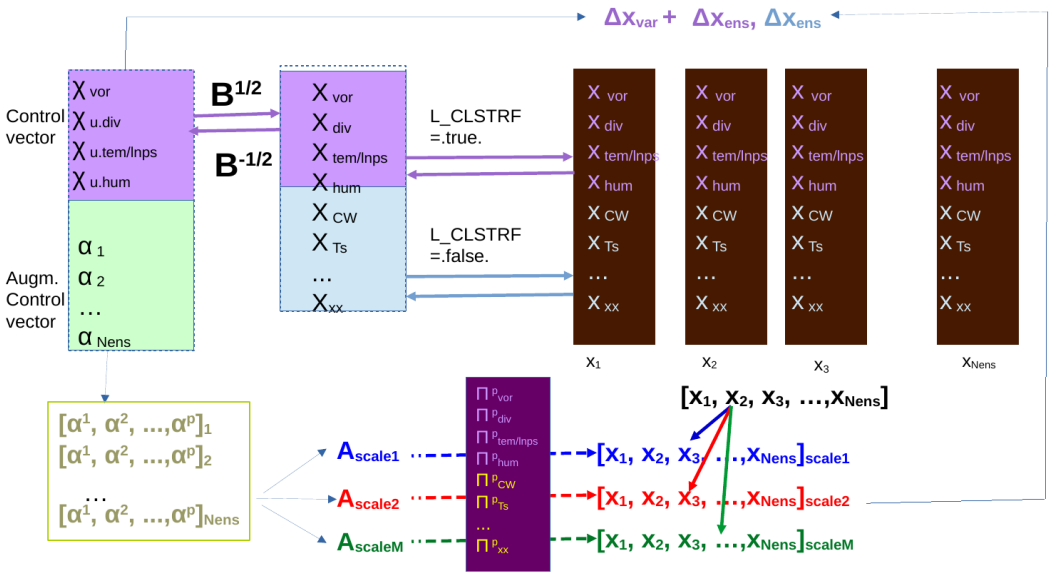

Figure 5.1. The schematic representation of the extended control variable approach to compute skin temperature increment

6.3 Further considerations

The following consideration should be taken into account:

- The quality of the error-of-the-day ensemble is essential to obtain the high-quality analysis increment of the skin temperature. The ensemble needs to be rich enough to capture the essential dependencies between the dynamical variables and the skin temperature. The only structures captured by the error-of-the-day ensemble can be used to determine the analysis increment. In addition, the error-of-the-day is estimated from the ensemble and the size of the ensemble plays an essential role. In the current experiments, the 20 high-resolution ensemble members have been used which add a substantial computational cost. The use of low-resolution ensembles has not been investigated.

- As a remedy of the limited ensemble size, the space-scale dependent localisation has been applied. The ensemble has been decomposed into three overlapping bands which imposes additional requirements on the memory usage. If more flexibility is needed and the larger number of overlapping bands is required the additional code optimization might be necessary.

- Although the introduction of the skin temperature into the extended control vector seems to be conceptually quite straightforward, substantial technical developments were needed. The integration of the land surface fields into the upper air variational

data assimilation framework is done by extending the functionalities of trajectory described in section 4.3. As it can be seen from discussions in section 4.4 some conceptual drawbacks or deficiencies in the implementation of the exchange of the information between the surface model and the atmosphere model through the trajectory might still be present.

- The surface temperature increment produced through the control variable approach seems to have a large amplitude at some locations. This induces a strong impact on the soil model through SEKF update using Jacobians. The substantial tuning of the couple atmosphere land surface data assimilation is still needed to obtain optimal performance. In addition, soil variables have a long memory and a longer spin-up period is needed in order to obtain consistency between the land surface and the atmosphere model states when the run is initiated from large scale boundary conditions.

7 Conclusions

One of the ultimate goals of the CERISE project is to design and implement a consistent land surface atmosphere data assimilation scheme to enhance efficiency in the utilisation of the satellite-derived data. This is a very challenging task because it requires an integration of information coming from systems that originally have been developed independently from each other. For the regional reanalysis Harmonie-Arome forecasting system is integrated with ISBA (Interactions between Soil Biosphere and Atmosphere) model within SURFEX (SURFace EXternalisé) platform to describe the energy and water exchange for natural surfaces. One complicating factor is that in the present version of the SURFEX platform there is no unique skin temperature variable defined in a consistent way for all involved surfaces although the skin temperature field is well defined for the upper air model. The work therefore has been focused on how to achieve more consistency in passing the information on skin temperature between the upper air and the surface models, how to identify the powerful and still affordable solution to enhance quality of the new generation reanalysis product, and to outline directions for further improvements to extract the full potential of observations derived from the satellite instruments.

The problem has been addressed from two different directions. The first one has been focused on constraining the land surface temperature field by using a weakly coupled land surface data assimilation, with the LETKF updating the surface variables and 3D-VAR updating the atmosphere. The coupling between the two components is done through a coupled land surface atmosphere forward model that provides the 3 hourly first guess field as for the next assimilation cycle. We apply the unified land data assimilation system developed in WP1 and reported in D1.3 and the machine learning observation operator from T1.4 (reported in D1.4) to assimilate AMSR-2 brightness temperature in addition to the screen level observations assimilated in the reference experiment. The assimilation of AMSR-2 provides a small but consistent improvement in upper air and the surface scores regarding the reference experiments except the coastal areas where the bias can be seen. Further tuning of the system is required in order to explore the scheme to its full potential (masking of AMSR-2 observations by the distance to the sea, tuning of observation error variance and the horizontal influence radius). The validation of soil analysis against independent measurements is not straightforward. The reference experiment seems to have slightly larger ACC scores but provide a smoother time evolution of the soil temperature that is more consistent with the evolution shown by the independent observations.

The second direction has been focused on the algorithmic developments of the data assimilation system to obtain a more consistent exchange of the information between the upper air and the surface model. The outer-loop HARMONIE-Arome 4D-Variational framework is evaluated on the ability to communicate surface temperature information between the upper-air and surface models. The communication between Earth-system components happens when computing the trajectory, which is basically a coupled forward forecast model along the assimilation window, when the land surface and the atmosphere exchange the information each time step. Both systems apply their own data assimilation methodology but they exchange the input information used by each. The trajectory run in the first outer-loop is initiated from the land and the atmospheric analysis at the beginning of the assimilation window. The analysis departures are used to update the first-guess field in the next outer loop's minimization. Similarly, the land analysis within the second loop is set as the initial field for the corresponding trajectory run. At the same time the screen-level fields are re-diagnosed with the updated upper-air fields during the trajectory run. These updated fields are used as background state during the subsequent assimilation (optimal interpolation). In addition, the

Jacobians used in the second loop along the trajectory are recalculated. The detailed analysis shows a healthy behavior of the system with the solution from the second outer loop being more optimal than the solution from the first outer loop. However, the investigation indicates a possible large-scale error or biases present in the solution degrading the quality of the temperature forecasts. More investigations are needed to understand to what extent the exchange of the information between land and surface components contribute to the problem: Is there a conceptual issue with the exchange of the information between land surface and atmosphere in the HARMONIE forecasting system when the large-scale systematic biases affect components? Or are there deficiencies in the implementation?

The upper air scheme is further extended by the functionality of the variational data assimilation scheme by introducing the extended control variable approach. The extended control vector approach allows to integrate the forecast error-of-the-day statistics derived from the ensemble evolution into the variational data assimilation framework and utilise dependencies built by the model between different model components. Each ensemble member is integrated by the coupled forward atmosphere land surface model, when the HARMONIE-Arome atmosphere model and the land surface ISBA-Dif model exchange the information each time step. This methodology allows to obtain an analysis correction to the skin temperature consistent with the upper air data assimilation and pass it to the surface data assimilation scheme. As a result, tiny balances and dependencies are built between all model components. Even if the implementation is conceptually straightforward the substantial technical developments are needed. The scheme is computationally heavy if the cost of the ensemble integration is considered. The integration of the surface information into the variational data assimilation is done through extending the functionalities of trajectory run and may suffer from the deficiencies in the implementation. The SEKF scheme needs to be adjusted in order to handle the surface temperature analysis increments provided by the upper air scheme in an efficient way. This includes limiting Jacobians to avoid a too strong update of deeper soil levels from the skin-temperature analysis increments and introduction of adaptive observation error variance for skin-temperature analysis increments.

The research done within this deliverable suggests the following steps to improve skin-temperature assimilation for regional reanalysis.

Step 1) use a weakly coupled assimilation of AMSR2 brightness temperature (through the forecast model) using 3D-Variational data assimilation; In parallel test outer-loop 4DVAR using a long enough spin-up period for assimilation of micro-wave radiance; Compare meteorological performance of the weakly coupled system against the meteorological performance of the outer-loop 4DVAR;

Step 2) resolve increment problem in the extended control variable skin-temperature analysis and tune the SEKF on the optimal performance (limiting Jacobians and adaptive observation error variance for skin-temperature analysis increments); Investigate system compatibility to run the LETKF surface data assimilation within the outer-loop Harmonie-Arome 4DVAR and within HybridEnVar.

Step 3) compare meteorological performance of skin temperature assimilation using extended control variable skin-temperature analysis and with the outer-loop 4DVAR coupling.

7.1 References

Barkmejer, J.., Lindskog, M., Gustafsson, N., Bojarova, J., Azad, R., Monteiro, I., Escribá, P., Whelan, E., Ridal, M., Sanchez Arriola ,J., Vignes, O., Stappers, R., Randriamampianina (2021). The HARMONIE-AROME 4DVAR. Technical Report. ALADIN-HIRLAM NL 16, Feb. 2021

Bengtsson, L., Andræ, U., Aspelien, T., Batrak, Y., Calvo, J., de Rooy, W., Gleesone, E., Hansen-Sass, B., Homleid, M., Hortal, M., Ivarsson, K.-I., Lenderink, G., Niemelä, S., Pagh Nielsen, K., Onvlee, J., Rontu, L., Samuelsson, P., Santos Muñoz, D., Subias, A., Tijm, S., Toll, V., Yang, X., & Ødegaard Køltzow, M. (2017). The HARMONIE-AROME model configuration in the ALADIN-HIRLAM NWP system. Monthly Weather Review, 145(5), 1919–1935. https://doi.org/10.1175/MWR-D-16-0417.1

Bojarova, J.. and Gustafsson, N. (2019). Relevance of the climatological background error statistics for mesoscale data assimilation. Tellus A : Dynamical Meteorology and Oceanography, 71, https://doi.org/10.1080/16000870.2019.1615168

Buehner, M.. and Shlyaeva, A. (2015). Scale-dependent background-error covariance localisation. Tellus A : Dynamical Meteorology and Oceanography, 67, https://doi.org/10.3402/tellusa.v67.28027

ECMWF (2022) CopERnIcus climate change Service Evolution, Project 101082139- CERISE-HORIZON-CL4-2021-SPACE-01 Grant Agreement, doi:10.3030/101082139

Entekhabi, D., Yueh, S., O'Neill, P., and Kellogg, K.: SMAP Handbook, JPL Pasadena, CA, USA, 400–1567, 2014.

Gustafsson N., Bojarova J. and Vignes 0. (2014) A hybrid variational data assimilation for the HIgh Resolution Limited Area Model, Nonlinear Processes in Geophysics, 21, 303-232 https://doi.org/10.5194/npg-21-303-2014

Hunt B. R., Kostelich E. J. and Szunyogh I. (2007) Efficient data assimilation for spatiotemporal chaos: A local ensemble transform Kalman filter, Physica D: Nonlinear Phenomena, 230, 1–2, 112-126, https://doi.org/10.1016/j.physd.2006.11.008.

Kerr, Y., Waldteufel, P., Wigneron, J.-P., Delwart, S., Cabot, F., Boutin, J., Escorihuela, M.-J., Font, J., Reul, N., Gruhier, C., Juglea, S., Drinkwater, M., Hahne, A., Martin-Neira, M., and Mecklenburg, S.: The SMOS Mission: New Tool for Monitoring Key Elements of the Global Water Cycle, P. IEEE, 98, 666–687, 2010

Noilhan J. and Mahfouf J.-F. (1996) The ISBA land surface parameterisation scheme, Global and Planetary Change, 13, 1–4, 145-159, https://doi.org/10.1016/0921-8181(95)00043-7.

Sakov, P., & Sandery, P. (2017). An adaptive quality control procedure for data assimilation. *Tellus A: Dynamic Meteorology and Oceanography*, *69*(1), 1318031.

Seity Y., Brousseau P., Malardel S., Hello G., Benard P., Bouttier F, Lac, C. and Masson V. (2011) The AROME-France convective scale operational model. Monthly Weather Review,

139(2), 976–991.

Tippett M. K., Anderson J. L., Bishop C. H., Hamill T. M. and Whitaker J. S. (2003) Ensemble Square Root Filters. Mon. Wea. Rev., 131, 1485–1490, https://doi.org/10.1175/1520-0493(2003)131<1485:ESRF>2.0.CO;2.

Thépaut J.-N. and Courtier P. (1991) Four-dimensional variational data assimilation using the adjoint of a multilevel primitive-equation model. Quart. J. Roy. Meteor. Soc., 117, 1225–1254, doi:10.1002/qj.49711750206.

Document History

Version	Author(s)	Date	Changes
0.1	Jelena Bojarova, Jostein Blyverket, Åsmund Bakketun, Mehdi Eshagh, José Manuel Faúndez Alarcón	5/12/2025	Initial version
1.0	Jelena Bojarova, Jostein Blyverket, Åsmund Bakketun, Mehdi Eshagh, José Manuel Faúndez Alarcón	Dec 2025	Updated after review comments

Internal Review History

Internal Reviewers	Date	Comments
Isabel Trigo (IPMA), Filipe Aires (ESTELLUS)	Dec 2025	Initial version